Surface Circulation in the Solomon Sea Derived from Lagrangian Drifter Observations*

HRISTINA G. HRISTOVA

Joint Institute for the Study of the Atmosphere and Ocean, University of Washington, Seattle, Washington

WILLIAM S. KESSLER

NOAA/Pacific Marine Environmental Laboratory, Seattle, Washington

(Manuscript received 19 May 2011, in final form 19 September 2011)

ABSTRACT

Velocity measurements from satellite-tracked surface drifters collected between 1994 and 2010 are used to map the surface circulation in the Solomon Sea, the last passageway for waters of subtropical origin flowing northward toward the equator, where they replenish the Pacific warm pool. Pseudo-Eulerian statistics of the drifter observations show a strong seasonal cycle in both the mean circulation and the eddy kinetic energy in the region. The circulation is characterized by a strong northward flow from June to November (the season of strong southeasterly trade winds over the Solomon Sea) and a mostly southward flow with increased variability from December to May (when the winds over the sea are weak). The seasonal velocity signal has the largest magnitude narrowly along the double western boundary formed by the eastern coastlines of New Guinea and the Solomon Islands, suggesting that direct wind driving with its much larger spatial scales is not the main influence. In addition, the surface circulation exhibits substantial interannual variability of magnitude comparable to that of the seasonal cycle with velocity and temperature anomalies consistent with changes in the western boundary current acting to compensate for the discharge and recharge of the Pacific warm pool during ENSO.

1. Introduction

The Solomon Sea in the southwest Pacific Ocean provides a western boundary connection between the subtropics and the equator. Waters of subtropical origin carried west by the South Equatorial Current (SEC) transit through the Solomon Sea and join the equatorial circulation, feeding the equatorial undercurrent and replenishing the Pacific warm pool (Gouriou and Toole 1993; Fine et al. 1994). Because surface ocean conditions along the equator determine the location of deep atmospheric convection and thus influence the development of El Niño events, changes in either the amount or properties of the waters coming through the Solomon Sea have the potential to create global-scale feedbacks (Gu and Philander 1997; McPhaden and Zhang 2002; Matei et al. 2008).

Because of its remoteness, in situ observations in the Solomon Sea are few and scattered in time and do not provide a complete picture of the mean circulation or its variability (Butt and Lindstrom 1994; Andrews and Clegg 1989; Murray et al. 1995; Cravatte et al. 2011). Global datasets, such as sea surface altimetry (Melet et al. 2010b) or Argo, are of limited utility because of the intricate geography of the region with numerous islands, reefs, and shallow passages. Recently, efforts have been put forward toward a more consistent monitoring of the southwest Pacific with coordinated glider missions, hydrographic cruises, and mooring deployments as part of the Climate Variability and Prediction (CLIVAR) Southwest Pacific Ocean Circulation and Climate Experiment (SPICE) international program (Ganachaud et al. 2008).

Because of the great interest to the Pacific circulation and climate, it is useful to expose and utilize existing historical observations for this data-sparse region as fully as possible. Here, we describe the surface circulation of

* Joint Institute for the Study of the Atmosphere and Ocean Contribution Number 1858, and Pacific Marine Environmental Laboratory Contribution Number 3678.

Corresponding author address: Hristina G. Hristova, NOAA/PMEL, 7600 Sand Point Way NE, Seattle, WA 98115.
E-mail: hristina.hristova@noaa.gov

DOI: 10.1175/JPO-D-11-099.1

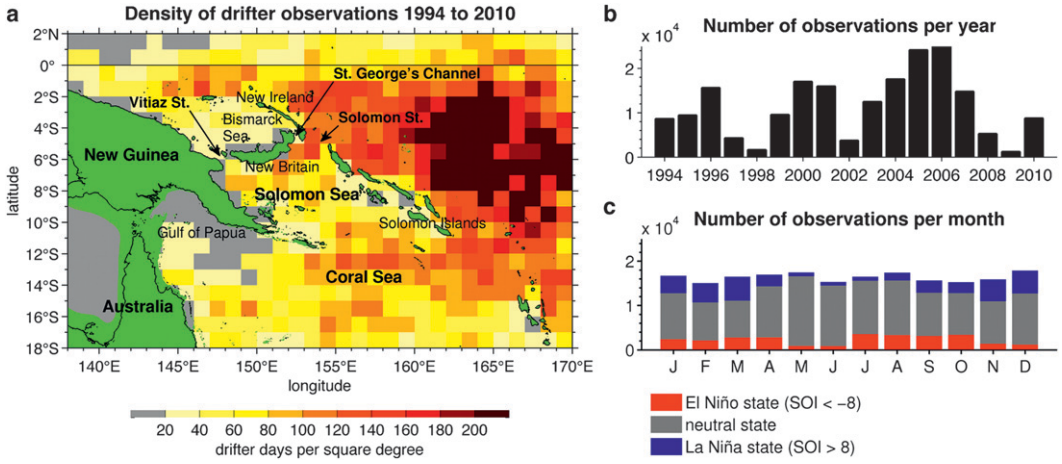

FIG. 1. (a) Density of drifter observations in the southwest Pacific Ocean during the 17-yr period from 1994 to 2010. Landmasses and depths shallower than 15 m are colored in green. The number of drifter velocity observations (b) per year and (c) per month. For each month, the number of observations is colored depending on the ENSO state (El Niño/neutral/La Niña), as indicated by the monthly value of the Southern Oscillation Index (SOI).

the Solomon Sea using the Global Drifter Program (GDP) dataset (Niiler et al. 1995; Niiler 2001) that uniquely samples close to coastlines and in narrow straits, regions poorly covered by remote techniques. Only in recent years has the number of drifter observations in the southwest Pacific become adequate to allow a robust representation of the small-scale patterns of the local circulation (e.g., Choukroun et al. 2010). Using the 17 most recent years of the drifter record, we show that surface drifters enhance the hydrological and satellite observations in the vicinity of the Solomon Sea by providing a realistic climatological description of the local surface circulation and offering insights into its mesoscale and interannual variability.

2. Data

GDP consists of an evolving fleet of satellite-tracked drifting buoys that follow the water motion at a nominal depth of 15 m. After quality control and kriging interpolation (Hansen and Poulain 1996), 6-hourly time series of drifter location, velocity, temperature, and associated interpolation errors are produced by the GDP Drifter Data Assembly Center (http://www.aoml.noaa.gov/phod/dac).

Here, we study a subset of the GDP velocity collection covering the Solomon Sea region (18°S–2°N, 138°–170°E) during the 17-yr period from 1994 to 2010. Velocity measurements from drifters that have lost their drogue or those with position interpolation error larger than 0.05° are excluded (10% of the total data points). Prior to analysis, the diurnal and tidal cycles in the measurements were removed by smoothing the data along drifter trajectories.

3. Spatial and temporal coverage of the data

The southwest Pacific is only moderately sampled by drifters, and their spatial and temporal coverage is not homogeneous. A total of 513 drifters have transited through the region of interest between 1994 and 2010, with only 97 passing through the Solomon Sea itself. The resulting average density of velocity observations for the region is 80 drifter days per square degree, or 1/3 less than the value of 120 for the tropical Pacific as a whole.

East of the Solomon Islands, the density of observations exceeds that inside the Solomon Sea by a factor of 2–3 (Fig. 1a). This reflects a combination of deployment history (90% of the drifters in the southwest Pacific have been released in the 5°S–5°N equatorial band north and east of the Solomon Sea) and subsequent drifter pathways (with the Solomon Islands acting as a barrier to the generally westward drifter propagation).

Of the total of 97 drifters that have sampled inside the Solomon Sea, none has been released within the sea itself. Instead, approximately one-third (35 drifters) entered the sea from the south through the Coral Sea, and two-thirds (61 drifters) entered from the east, with 39 drifters entering via Solomon Strait and the remaining 22 drifters squeezing in through the various gaps in the Solomon Islands chain. From the north, only one drifter entered the Solomon Sea through St. George's Channel and none entered through Vitiaz Strait. For half of the drifters that entered the Solomon Sea, the last reported position was inside the sea; the remaining half spent, on average, 50 days in transit.

To the south, in the Coral Sea, very few drifters venture into the Gulf of Papua and no drogued drifter transits

into the Indian Ocean through Torres Strait between Australia and New Guinea, probably because it is extremely shallow (<10 m). The coverage, especially in the Gulf of Papua and the Great Barrier Reef, is slightly better if drifters that have lost their tethered drogue are included (Choukroun et al. 2010). However, the velocities of such drifters are harder to interpret because of wind slippage and are excluded from our study.

The number of drifter observations is nearly uniform among months but varies significantly from year to year (Figs. 1b,c). Taking the ENSO state into account, as indicated by the 5-month weighted average of the Southern Oscillation index (SOI), indicates that about 14% of the observations were collected during El Niño, 18% were collected during La Niña, and 68% were collected during the neutral state.

The uneven spatial sampling undoubtedly hampers estimation of the complete circulation in the region. The majority of the Solomon Sea has adequate coverage with at least 20 drifter days per square degree, but drifters are of little help in places of poor sampling, such as the Gulf of Papua and the Bismarck Sea. Elsewhere, the temporal sampling by the 17-yr-long record is adequate to describe the circulation variations on annual time scales and to attempt an estimation of its interannual variations on ENSO time scales.

4. Methodology

Obtaining pseudo-Eulerian velocity estimates from the Lagrangian drifter velocities requires spatial averaging. We adopted the following approach to satisfy the need for a fine spatial resolution in the Solomon Sea despite the modest data density.

The data were analyzed on a ½° latitude–longitude grid. At each grid point an ellipse was defined with area of 4 times the grid resolution and axes oriented and scaled by the local velocity variance (Johnson 2001). The elliptical bins were therefore found to be elongated zonally near the equator and along the coastline near landmasses, thus improving the representation of coastal and equatorial currents. The overlap of the bins means that each drifter velocity contributes to the Eulerian velocity estimate at several (on average four) grid points, equivalent to spatial smoothing along the direction of maximum variance, thus preserving the sharpness of coastal currents. No velocity was computed for bins with data density less than 20 drifter days per square degree (gray shading in Fig. 1a).

All drifter measurements within a bin were treated as a time series and fitted with a mean value, an annual harmonic (1 cycle per year), a coefficient proportional to the SOI, and a residual eddy component. Especially in regions of modest sampling, fitting these coefficients to the data in each bin is superior to a simple bin averaging because it helps avoid seasonal bias of the mean without sacrificing spatial resolution or coverage (Lumpkin 2003).

We chose not to include a semiannual harmonic in the decomposition because in a large portion of the bins (especially within the Solomon Sea) the number of drifter observations is only moderate; we found that including a semiannual harmonic does not result in a better seasonal cycle fit. The annual harmonic by itself is sufficient to capture the essence of the two main seasons for the Solomon Sea (section 6a). The incorporation of a coefficient proportional to the SOI aims to reduce contamination of the mean and seasonal velocity estimates by the strong interannual ENSO variability characteristic of the tropical Pacific (Johnson 2001; Melet et al. 2010b).

5. Mean circulation

The drifter-estimated mean surface velocity includes both a geostrophic and an Ekman component. We compared our mean field to an independent estimate of the total surface velocity from the ⅓° Ocean Surface Current Analysis–Real Time (OSCAR) product (Bonjean and Lagerloef 2002). OSCAR uses a quasi-linear model and direct observations of sea surface height, temperature, and surface vector wind from remote sensing and in situ instruments (but not drifters) to estimate the surface velocity at 5-day intervals. For comparison purposes, we interpolated the 1994–2010 OSCAR velocity to the ½° drifter grid and performed the same decomposition into mean, seasonal, and SOI components.

The drifter and OSCAR mean surface velocity estimates share the same general features away from landmasses (Fig. 2). The circulation east of the Solomon Islands is dominated by the broad westward SEC, representing the westward limb of the South Pacific subtropical gyre. The SEC is strongest in two bands a few hundred kilometers wide centered near 3° and 14°S. The southern SEC branch extends through the Coral Sea all the way to Australia, whereas the equatorial branch splits at Solomon Strait, with part deflected north of New Ireland and part through the Solomon Sea south of New Britain.

One obvious advantage of the drifter-estimated velocity is the better coastal and strait coverage; because OSCAR is based on satellite observations, there are no data close to land, which for the southwest Pacific means a large portion of the Solomon Sea, including the important Vitiaz Strait connection to the equator. A better coastal coverage from altimetry can be obtained if the along-track satellite data is considered, in which case

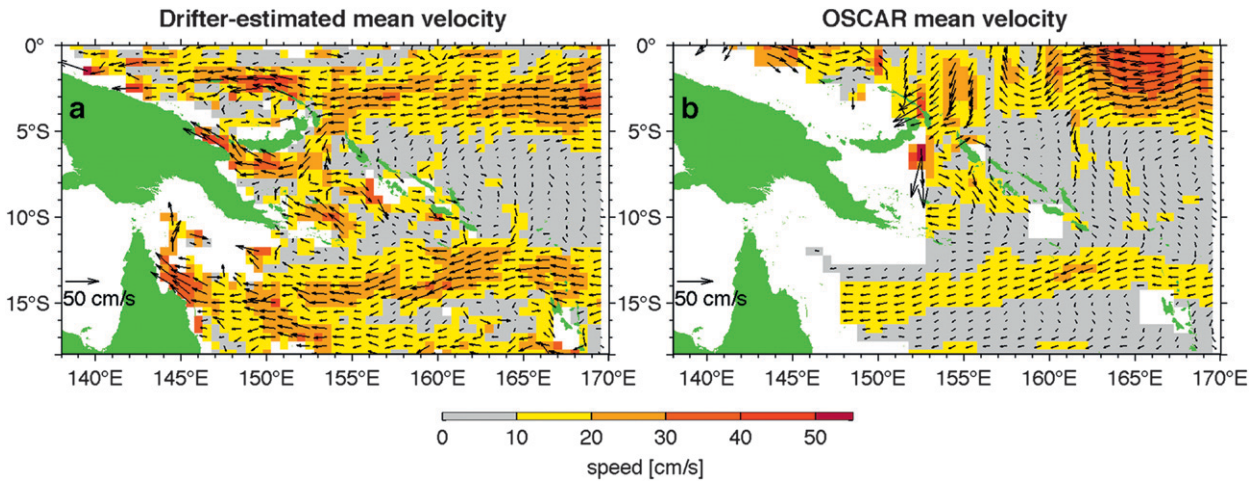

FIG. 2. Comparison of the annual-mean surface velocity estimated from (a) the GDP dataset and (b) the 1/3° OSCAR product (based on remote sensing data). Every other vector in x is plotted.

cross-track geostrophic current anomalies can be computed for the few tracks that pass through the Solomon Sea (Melet et al. 2010b).

At Solomon Strait, the drifters indicate mean surface flow into the sea, which then parallels the coast of New Britain and exits through Vitiaz Strait. The inward direction of the drifter-estimated surface flow at Solomon Strait is consistent with that obtained by averaging direct measurements from historical shipboard acoustic Doppler current profiler (SADCP) data (Cravatte et al. 2011, their Fig. 8). At the southern entrance of the Solomon Sea, drifters, OSCAR (where available), and SADCP (Cravatte et al. 2011) show equatorward flow around the southeastern tip of New Guinea and through its Woodlark Archipelago; this is the New Guinea Coastal Current (NGCC). There is a southward flow in the eastern part of the basin and within the gaps of the Solomon Islands chain, again consistent with direct measurements (Cravatte et al. 2011, their Fig. 4) and model results (Melet et al. 2010a).

The drifter-estimated velocity has generally stronger magnitude than OSCAR. We think this is more realistic because the drifters better sample the swift, narrow boundary currents. The small bin size and the present method of focused spatial interpolation (using overlapping ellipses oriented by the local velocity variance) results in less smoothing across islands and better resolves the narrow boundary currents that carry much of the transport, compared to OSCAR and other global-drifter-derived velocity climatologies (Lumpkin and Garraffo 2005). The drifter-estimated speeds of 20–60 cm s^{-1} in the surface boundary currents are within the range of directly measured speeds (Butt and Lindstrom 1994; Murray et al. 1995; Cravatte et al. 2011).

6. Seasonal variations

a. Surface currents

The seasonal cycle in the southwest Pacific is dictated by the annual march of the intertropical convergence zone (ITCZ) and South Pacific convergence zone (SPCZ) and, in the west, by monsoon winds (Kessler and Gourdeau 2007). The temperature variations over these low latitudes are minimal, but there are pronounced seasonal changes in the wind stress and precipitation. The two main seasons in the Solomon Sea are the dry, strong-trade season (June–November), and the wet, weak-trade season (December–May) (Figs. 3a,b). During the wet season, the SPCZ is found over the Solomon Sea and the seasonal-mean winds weaken, reversing direction and becoming northwesterly east of the Solomon Islands and along the equatorial coast of New Guinea west of Vitiaz Strait.

In sharp contrast to the wind stress that has large spatial scales, the drifters indicate seasonal surface velocity anomalies of much smaller scale. The largest magnitude anomalies are usually within 200 km of the coast where they reach 15–30 cm s^{-1}. The June–November strong-trades season is characterized by a westward anomaly in the interior Pacific between 8°S and 12°S that splits on reaching the Solomon Islands chain at about 162°E (Fig. 3c). Part of the anomalous flow enters the Solomon Sea from the south and through gaps in the Solomon Islands chain and then can be traced equatorward through Vitiaz Strait and along the equatorial coast of New Guinea. Another part of the anomalous flow turns north along the eastern coast of the Solomon Islands. It is most prominent within 100–150 km from the coast north of 8°S and can be traced equatorward past New Ireland.

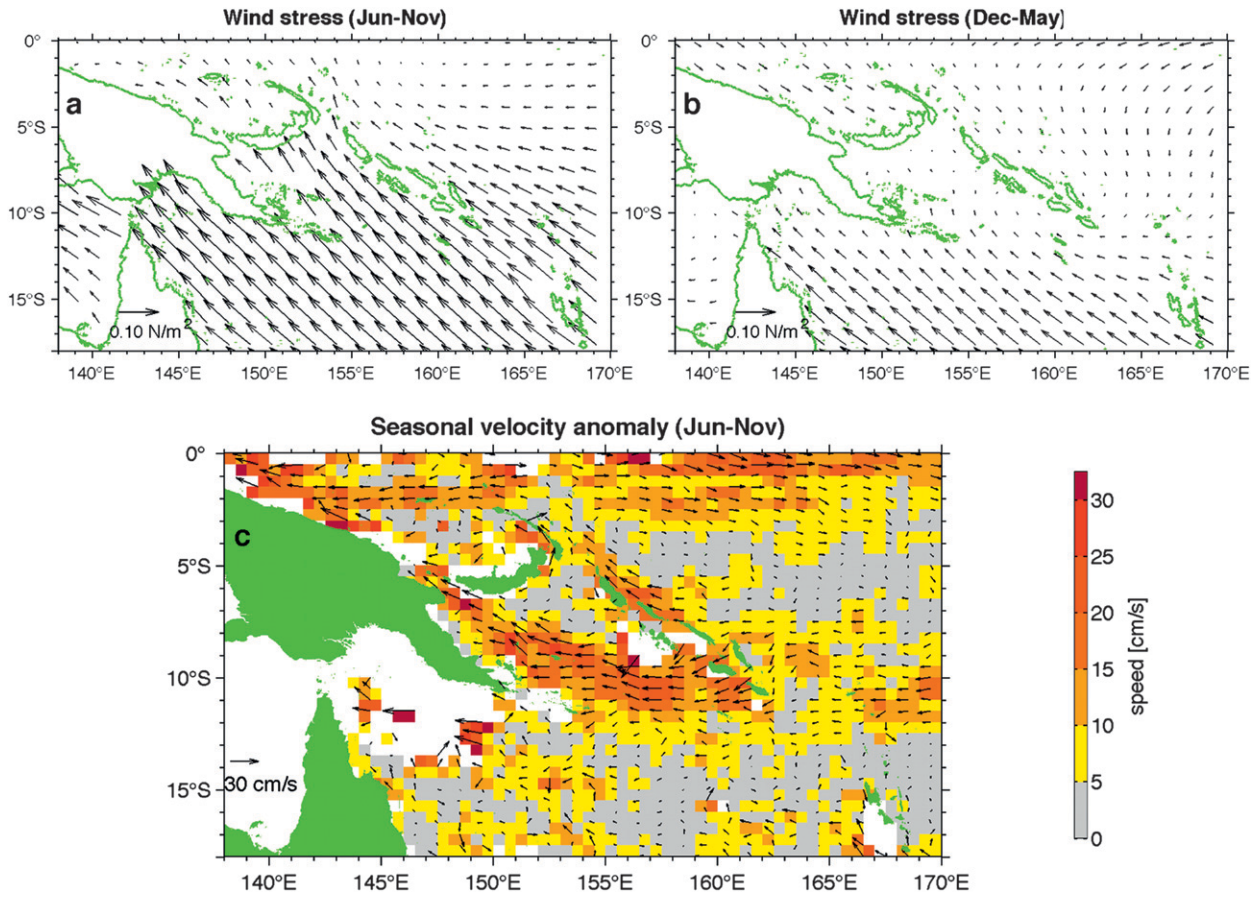

FIG. 3. Seasonally averaged wind stress over the Solomon Sea during (a) June–November (the strong-trades season) and (b) December–May (the weak-trades season), based on the wind climatology by Risien and Chelton (2008). (c) Drifter-estimated surface velocity anomaly for June–November. Because in our analysis the seasonal cycle is represented by a sine function, the December–May anomalies have the same magnitude but opposite direction. For the surface velocity, every other vector in x is plotted.

Seasonal geostrophic current anomalies computed from altimetry show a generally similar pattern and magnitude but with less boundary intensification and lacking the coastal signal on the eastern side of the Solomon Islands (Melet et al. 2010b, their Fig. 6). These differences can be probably attributed to the difficulty of interpreting altimetric SSH measurements in proximity to the coastline and the subsequent finite differencing to obtain the geostrophic current.

Although the seasonal variation of the surface circulation estimated from the drifters tends to be in the direction of the winds, the lack of small-scale spatial structure in the forcing field suggests that it is not a simple wind-driven response. Instead, a more likely explanation is that the drifters are sampling better the narrow boundary currents. This is corroborated by the global 1° drifter climatology by Lumpkin and Garraffo (2005) that provides a decomposition of the surface drifter-estimated velocity into total and Ekman-removed components. In the southwest Pacific, the Ekman drift is southwestward at roughly 90° from the prevailing southeasterly winds and is strongest between July and October, when the southeasterly winds are also at their strongest. Although at specific locations the estimated Ekman currents can have magnitude comparable to the geostrophic currents, their means and seasonal anomalies are virtually uniform over the entire region and cannot explain the small-scale spatial structure found in the surface velocity field.

The seasonal velocity anomalies in the boundary currents are on the same order as the mean, implying that the surface boundary currents vary significantly during the year. When the seasonal anomaly is superimposed on the mean, the June–November strong-trades circulation is characterized by a large SEC inflow into the Coral Sea and a strong equatorward flow both through the Solomon Sea and along the eastern coast of the Solomon Islands north of 8°S (Fig. 4a). In this season, the NGCC is at its maximum with speeds of 40–50 cm s^{-1} and can be traced through Vitiaz Strait and along the equatorial coast of

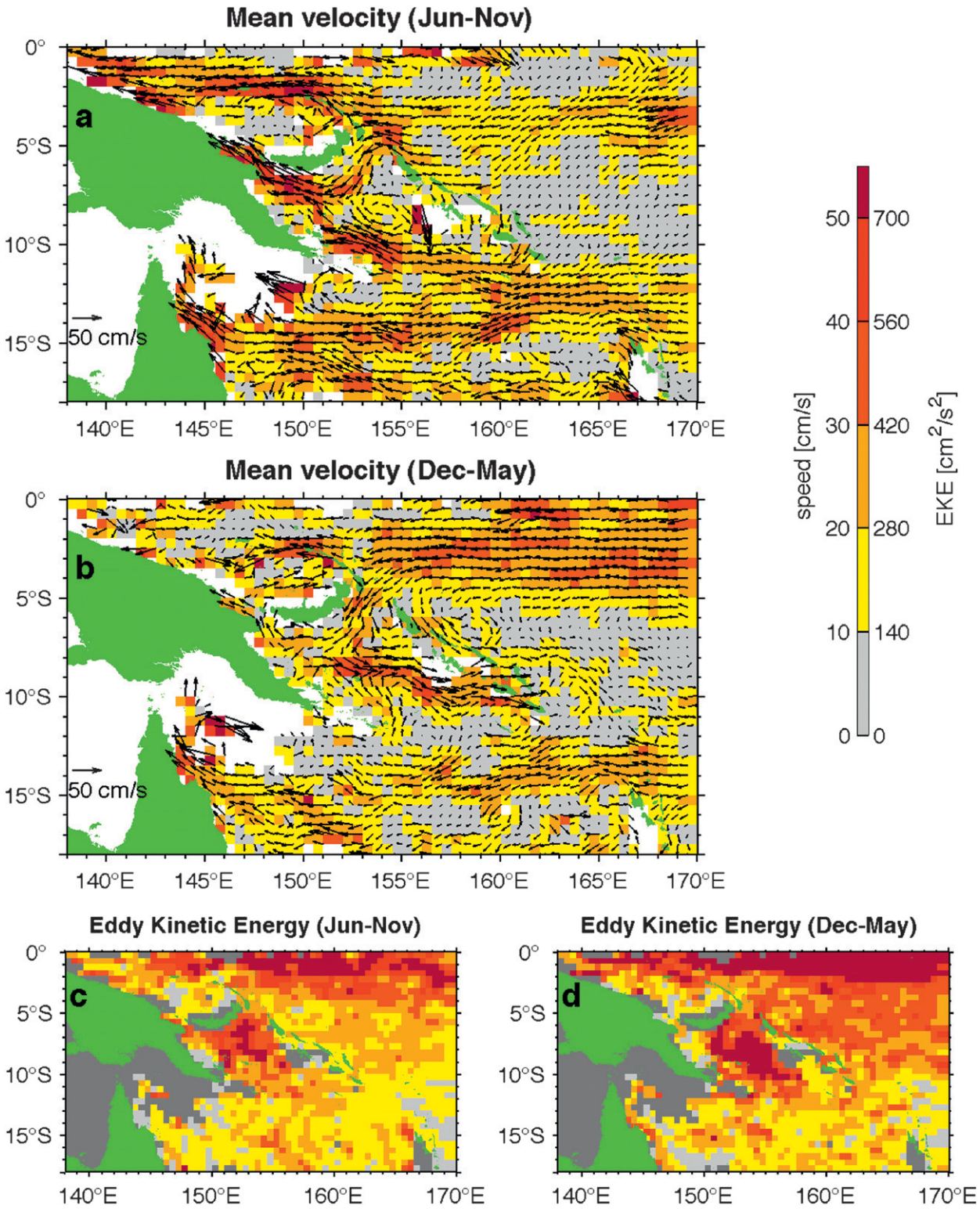

FIG. 4. Drifter-estimated surface velocity and mean EKE averaged seasonally: (a),(c) June–November average (the strong-trades season) and (b),(d) December–May average (the weak-trades season).

New Guinea (Murray et al. 1995; Ueki et al. 2003). In the northern Solomon Sea away from the coast, the June–November circulation is dominated by a cyclonic (clockwise) recirculation cell with a diameter of about 400–450 km centered at 9°S, 154°E.

During the December–May weak trades, on the other hand, the SEC is strong near the equator, whereas the eastward (10–20 cm s^{-1}) South Equatorial Countercurrent (SECC) is found in the 8°–10°S band east of the Solomon Islands (Chen and Qiu 2004) (Fig. 4b). In this season, the flow in the Solomon Sea and east of the Solomon Islands is reversed to be southward, and the only equatorward surface flow is the weakened (by about a factor of 2) NGCC along the east coast of New Guinea exiting through Vitiaz Strait. This is consistent with previous measurements that indicate a significant decrease in Vitiaz Strait equatorward transport that can even reverse direction at the surface during December–February (the northwesterly monsoon season) (Murray et al. 1995; Cravatte et al. 2011); however, none of the 15 drifters in Vitiaz Strait went south (into the sea).

Although there is a strong (15–20 cm s^{-1}) seasonal signal in the surface velocity in both Vitiaz Strait and St. George's Channel, this is less true in Solomon Strait, where the seasonal velocity anomaly is on the order of 5–10 cm s^{-1}, much less than the mean of 20–30 cm s^{-1} (Figs. 3c, 2a). As a result, the drifter-estimated surface velocity through Solomon Strait is westward (into the sea) year-round. Within this overall picture, some additional details can be seen. During the December–May weak-trades season, the surface current in Solomon Strait is maximum (20–30 cm s^{-1}) on the New Ireland side of the strait, whereas it weakens and can occasionally reverse direction near the Solomon Islands side of the strait, consistent with previous measurements (Cravatte et al. 2011) (Fig. 4b). Of the 45 drifters that have traveled through Solomon Strait during the 17-yr period, only one exited the Solomon Sea near the Solomon Islands (in late November). During the June–November strong-trades season, on the other hand, the surface current in Solomon Strait is maximum (20–30 cm s^{-1}) on the Solomon Islands side of the strait, whereas the drifters indicate a bifurcation and an eastward (10 cm s^{-1}) current along the New Britain coast that exits through St. George's Channel toward the Bismarck Sea (Fig. 4a). A similar pattern of circulation but with the bifurcation much more pronounced has been described previously from SADCP data (Cravatte et al. 2011).

b. Mean eddy kinetic energy

As a measure of the circulation mesoscale variability, we computed the mean eddy kinetic energy (EKE) by time averaging the square of the residual eddy drifter velocities u' and v' remaining after removing the mean, seasonal, and ENSO cycles from the total velocity time series in each bin, $\mathrm{EKE} = (1/2)(\overline{u'^2} + \overline{v'^2})$. Interannual velocity variations in the tropical Pacific are as important as seasonal (as we will show in the next section and as indicated by altimetry; Melet et al. 2010b), so it is essential to remove the ENSO dependence by filtering or other means as here; otherwise, larger values for the EKE are obtained that include a low-frequency contribution.

Previous studies indicate high mesoscale variability of the circulation in the Solomon Sea, especially in the vicinity of Solomon Strait (Cravatte et al. 2011; Melet et al. 2010b). In agreement, the drifters also single out the Solomon Sea as a region of maximum EKE (other than the equator) where values exceed 700 cm^2 s^{-2} (Figs. 4c,d). Outside the Solomon Sea, the larger EKE east of the Solomon Islands during December–May (Fig. 4d) likely reflects the enhanced eddy generation through barotropic instabilities of the SECC, at its strongest during March–April (Qiu and Chen 2004).

There is a clear seasonal modulation of the EKE in the Solomon Sea. Analysis of the geostrophic current variability from altimetry shows that the EKE is maximum during the first half of the year (Melet et al. 2010b). What the drifter record reveals in addition is that not only the magnitude but also the location of maximum variability changes seasonally. High variability is confined to the northern Solomon Sea during June–November, when the mean flow is strongly toward the equator (Fig. 4c). During December–May, on the other hand, when the mean flow is mostly to the south and less spatially coherent, the variability spreads over the entire sea and is generally stronger (Fig. 4d).

Time series of bimonthly EKE spatially averaged over the southwest Pacific (2.5°–12.5°S, 147°–170°E) shows maximum values from March to June and lower values during the remainder of the year (Fig. 5). There is a near doubling of the level of EKE in the region (from 300 cm^2 s^{-2} in July/August to 540 cm^2 s^{-2} in March/April). This reflects both the enhanced variability in the Solomon Sea and the SECC instabilities east of the Solomon Islands that develop during that season. A similar seasonal cycle of the EKE is found from OSCAR surface velocity. Values are however lower in OSCAR by 30%–40%, partially because large portion of the Solomon Sea velocity field is missing in that dataset (Fig. 2a).

Small-scale structure in the wind stress curl field is associated with enhanced eddy generation in the wake of several islands in the tropical Pacific (e.g., Chavanne et al. 2002; Qiu et al. 2009). The situation of the Solomon Islands is different, however. They are oriented nearly in the direction of the prevailing southeasterly trade winds,

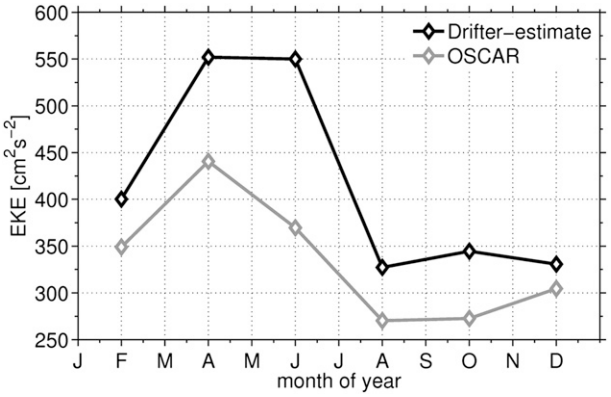

FIG. 5. Seasonal cycle of the mean EKE computed from the GDP dataset and OSCAR, spatially averaged over the southwest Pacific (2.5°–12.5°S, 147°–170°E).

which is not efficient for creating small-scale curl signal on their downwind side. Also, because the Solomon Sea is situated at the western boundary of the ocean, there is not a stretch of open ocean where the curl signal can propagate and lead to pronounced eddy generation through shear instabilities as for Hawaii (Chavanne et al. 2002) or Vanuatu (Qiu et al. 2009).

There are other factors that can account for the enhanced surface current mesoscale variability in the Solomon Sea compared to its surroundings. Interaction with topography, advection of eddies from the open ocean, and local instabilities all could possibly contribute to the high EKE in the Solomon Sea. In addition, the Solomon Sea is influenced by the Madden–Julian oscillation (period of 30–60 days) and is also situated at the northern edge of the South Pacific tropical cyclone track (season runs from November to April). This high-frequency wind variability might also result in enhanced surface current mesoscale variability in the Solomon Sea.

7. Interannual variations

On longer than annual time scales, the dominant signal in the tropical Pacific is the ENSO cycle (Ridgway et al. 1993; Melet et al. 2010b). In our analysis, the variations of the surface circulation associated with ENSO can be estimated from the spatial structure of the velocity coefficient proportional to SOI that was fitted to the drifter data in each bin. As a cautionary note, a linear regression on SOI can have drawbacks; for example, it implies a symmetric, no-lag response during El Niño and La Niña, which is likely an oversimplification (Melet et al. 2010a). However, given the relatively short record length, limited sampling, and the difficulty of choosing a suitable lag, this was the most straightforward approach in order to separate the ENSO from the seasonal signal in the drifter record.

The drifter-estimated ENSO velocity anomaly is of similar magnitude to the seasonal anomaly and has its strongest expression along the equator and within the Solomon Sea, where it reaches 20–40 cm s^{-1} (Fig. 6a). Note that most of the ENSO anomaly for the Solomon Sea is confined to the interior of the sea; there is no boundary-trapped signal east of the Solomon Islands as for the seasonal velocity anomaly (Fig. 3c).

During El Niño, the general direction of the anomaly in the Solomon Sea is such that it enhances the equatorward western boundary current, bringing more waters of subtropical origin toward the equator. Previous observations show strong ENSO transport variability in Vitiaz and Solomon Straits (Ridgway et al. 1993; Melet et al. 2010b; Cravatte et al. 2011). From the drifter record, we find only a weak (<10 cm s^{-1}) surface signal in Solomon Strait (outward anomaly during El Niño). There is not sufficient drifter sampling in Vitiaz Strait itself to reliably fit an ENSO coefficient. Examination of individual drifter tracks shows, however, that during El Niño the equatorward surface velocity in Vitiaz Strait is larger than its seasonal mean, consistent with what the earlier studies suggest.

Along the equator, the El Niño anomaly has the expected eastward direction, reflecting the slowdown and reversal of the normally westward surface equatorial current in response to the weakened trade winds. An eastward El Niño anomaly is found in the drifter observations as far west as 140°E along the equatorial coast of New Guinea. In the Pacific interior, the El Niño velocity anomaly is relatively weak but consistent with the increased influx of subtropical waters into the Solomon Sea. In the opposite phase, during La Niña (when the velocity anomalies have opposite sign to that in Fig. 6a), the normally westward surface equatorial current is strengthened, whereas the Solomon Sea equatorward surface current decreases and can even reverse direction to the south, draining waters from the equator.

These drifter-estimated velocity anomalies are consistent with the view that at ENSO time scales the low-latitude western boundary currents act opposite to the discharge/recharge of the equatorial warm pool volume (Lee and Fukumori 2003). Given that the drifters sample the surface (10–20 m) currents only, this suggests some degree of correlation between the surface and thermocline circulation anomalies, at least at these interannual time scales.

Associated with the ENSO velocity anomalies, there are corresponding ENSO temperature anomalies that we derived similarly from the drifter record. During El Niño, the temperature east of the Solomon Islands is warmer than usual by up to 1°C, reflecting the southward and eastward expansion of the warm pool (Fig. 6b). By

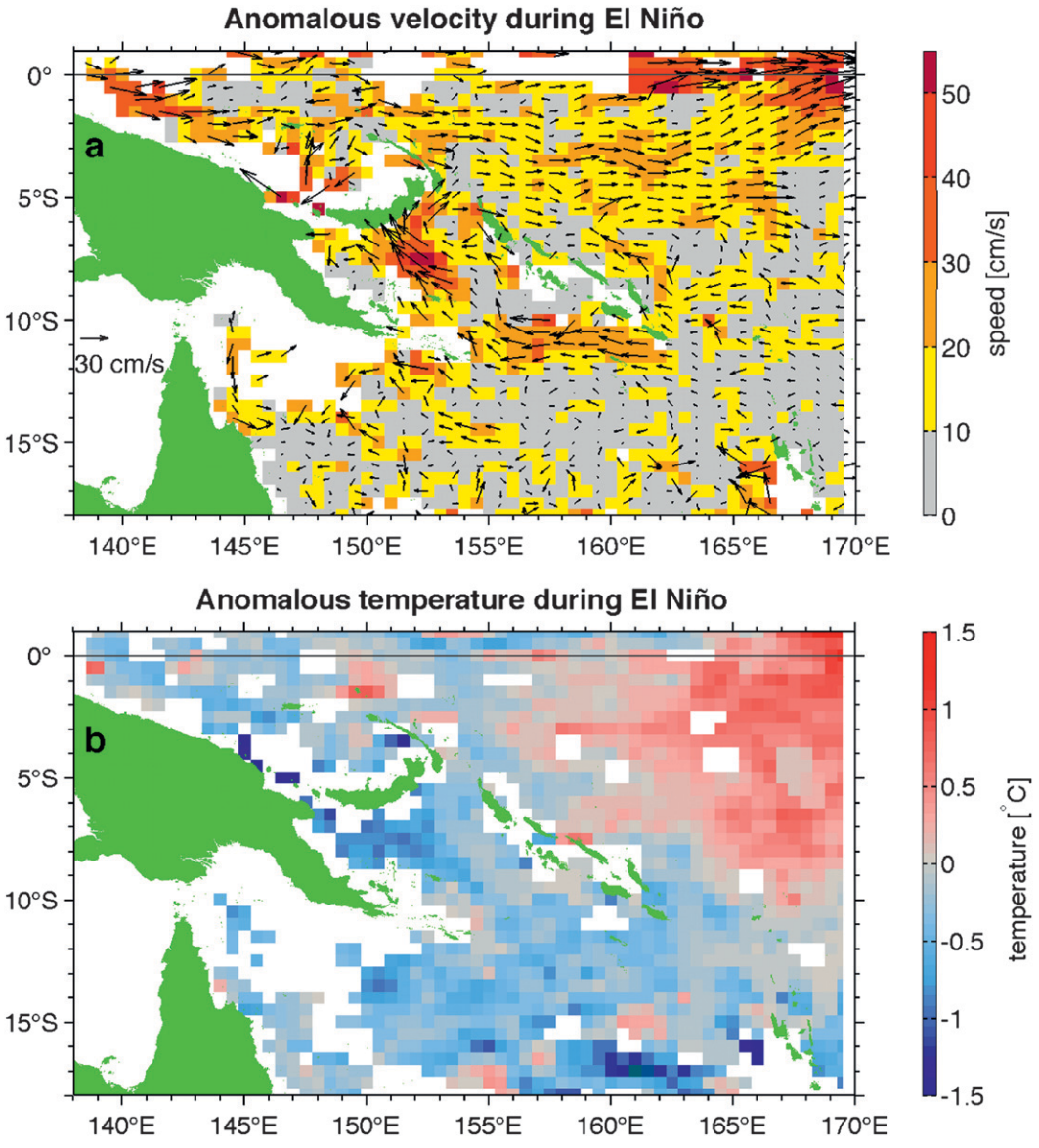

FIG. 6. Drifter-estimated anomalies for (a) the surface velocity and (b) the temperature associated with El Niño. The La Niña anomalies have reversed direction for the velocity and opposite sign for the temperature. For the velocity, every other vector in x is plotted.

contrast, the anomaly inside the Solomon Sea is of opposite sign. This is consistent with the idea that the surface flow in the Solomon Sea acts to compensate the equatorial changes; it brings northward cooler subtropical waters from farther south in the Coral Sea during El Niño when the warm pool spills eastward and warmer equatorial waters into the Solomon Sea during La Niña when the warm pool is rebuilding. Radiocarbon records from corals suggest similar changes in the surface water masses in the western Pacific, with time series from Nauru (just north of the Solomon Sea at 0.5°S, 166°E), showing a larger fraction of subtropical waters during El Niño events and a larger fraction of equatorial waters during La Niña events (Guilderson et al. 1998).

Similar to estimates from altimetry data (Melet et al. 2010b), the drifter record also points out to higher mesoscale variability in the Solomon Sea during El Niño events (not shown here). This is in contrast with the seasonal variations of the EKE; although, at the seasonal time scale, the stronger NGCC in June–November is associated with low EKE, at ENSO time scales the stronger NGCC during El Niño is associated with large EKE.

8. Summary

We used the 17 most recent years (1994–2010) of Lagrangian drifter observations from the Global Drifter Program (Niiler et al. 1995; Niiler 2001) to map the near-surface circulation in the Solomon Sea. The drifter data uniquely samples close to coastlines and in straits, which is crucial in this region, where much of the flow occurs in narrow boundary currents that are poorly sampled by remote techniques. Compared to other drifter studies that treat the large-scale circulation, special care was taken here of the Solomon Sea's particularities: the relatively modest drifter coverage and the need to avoid smoothing across landmasses in order to represent the circulation amid the numerous islands and narrow straits of the region.

With careful mapping, the drifters provide an enhanced description of the seasonal cycle of the surface circulation, improving the coverage and spatial detail compared to satellite-derived estimates (Bonjean and Lagerloef 2002; Melet et al. 2010b) and other direct measurements (Cravatte et al. 2011). Unlike results from altimetry, the drifters indicate that the seasonal surface velocity signal is focused narrowly along the double western boundary formed by the eastern coastlines of New Guinea and the Solomon Islands. The small-scale structure in the signal suggests that the seasonal variation of the surface circulation, although broadly consistent with the changing wind direction, is not a simple response to the winds that have much larger spatial scales.

During June–November (the season of strong southeasterly trades over the Solomon Sea), the northward NGCC is at its maximum (speeds of 40–50 cm s^{-1}), and a northward surface current is present along the eastern coast of the Solomon Islands. During December–May, on the other hand (when the trades over the sea are weak), the surface flow in the Solomon Sea and east of the Solomon Islands is reversed to be southward, and the only equatorward surface current is the weakened (10–30 cm s^{-1}) NGCC. Drifter estimates of the mesoscale EKE show that the maximum variability is confined to the northern Solomon Sea during June–November, when the mean flow is strongly toward the equator, whereas the variability spreads over the entire sea and is generally stronger during December–May, when the mean flow is mostly to the south and less spatially coherent.

The drifter coverage is marginal to resolve interannual and longer time scales. Nevertheless, the 17-yr record captures the major characteristics of the ENSO signature in the western Pacific. Unlike the seasonal velocity anomalies, the largest ENSO velocity signal is confined inside the Solomon Sea. The western boundary current through the Solomon Sea acts to compensate the equatorial changes, with increased subtropical transport toward the equator during El Niño events when the warm pool spills eastward and decreased transport during La Niña events when the warm pool is rebuilding (Lee and Fukumori 2003). Broad cooling during El Niño and warming during La Niña in the Solomon and Coral Seas shows the signature of these changes in the surface circulation.

One aspect not addressed here is Lagrangian statistics of the drifter data, such as velocity autocorrelations and spectra. Visual inspection of the drifter tracks suggests that those change seasonally as well. This complementary description of the mesoscale field can be a valuable additional information in assessing the realism of numerical models for the region.

Acknowledgments. The authors honor the memory of Peter Niiler, without whose vision, energy, and forcefulness there would have been no Global Drifter Program. We acknowledge the helpful comments from the two anonymous reviewers. The OSCAR data were obtained from JPL Physical Oceanography DAAC and developed by ESR. This publication is funded by NASA under JPL Subcontract 1377557 and the Joint Institute for the Study of the Atmosphere and Ocean (JISAO) under NOAA Cooperative Agreement NA10OAR4320148.

REFERENCES

Andrews, J. C., and S. Clegg, 1989: Coral Sea circulation and transports deduced from modal information models. *Deep-Sea Res.,* **36,** 957–974.

Bonjean, F., and G. S. E. Lagerloef, 2002: Diagnostic model and analysis of the surface currents in the tropical Pacific Ocean. *J. Phys. Oceanogr.,* **32,** 2938–2954.

Butt, J., and E. Lindstrom, 1994: Currents off the east coast of New Ireland, PNG and their relevance to regional undercurrents in the western equatorial Pacific Ocean. *J. Geophys. Res.,* **99** (C6), 12 503–12 514.

Chavanne, C., P. Flament, R. Lumpkin, B. Dousset, and A. Bentamy, 2002: Scatterometer observations of wind variations indiced by oceanic islands: Implications for wind-driven ocean circulation. *Can. J. Remote Sens.,* **28,** 466–474.

Chen, S., and B. Qiu, 2004: Seasonal variability of the South Equatorial Countercurrent. *J. Geophys. Res.,* **109,** C08003, doi:10.1029/2003JC002243.

Choukroun, S., P. V. Ridd, R. Brinkman, and L. I. W. McKinna, 2010: On the surface circulation in the western Coral Sea and residence times in the Great Barrier Reef. *Geophys. Res. Lett.,* **115,** C06013, doi:10.1029/2009JC005761.

Cravatte, S., A. Ganachaud, Q.-P. Duong, W. S. Kessler, G. Eldin, and P. Dutriuex, 2011: Observed circulation in the Solomon Sea from SADCP data. *Prog. Oceanogr.,* **88,** 116–130.

Fine, R. A., R. Lukas, F. M. Bingham, M. J. Warner, and R. H. Gammon, 1994: The western Pacific: A water mass crossroads. *J. Geophys. Res.,* **99** (C12), 25 063–25 080.

Ganachaud, A., and Coauthors, 2008: Southwest Pacific Ocean Circulation and Climate Experiment (SPICE)—Part II. Implementation plan. NOAA OAR Special Rep., CLIVAR Publication Series 133, 42 pp.

Gouriou, Y., and J. Toole, 1993: Mean circulation of the upper layers of the western equatorial Pacific Ocean. *J. Geophys. Res.,* **98** (C12), 22 495–22 520.

Gu, D. F., and S. G. H. Philander, 1997: Interdecadal climate fluctuations that depend on exchanges between the tropics and extratropics. *Science,* **275,** 805–807.

Guilderson, T. P., M. Kashgarian, and J. Southon, 1998: Radiocarbon variability in the western equatorial Pacific inferred from a high-resolution coral record from Nauru Island. *J. Geophys. Res.,* **103** (C11), 24 641–24 650.

Hansen, D. V., and P.-M. Poulain, 1996: Quality control and interpolations of WOCE–TOGA drifter data. *J. Atmos. Oceanic Technol.,* **13,** 900–909.

Johnson, G. C., 2001: The Pacific Ocean subtropical cell surface limb. *Geophys. Res. Lett.,* **28,** 1771–1774.

Kessler, W. S., and L. Gourdeau, 2007: The annual cycle of circulation of the southwest subtropical Pacific, analyzed on an ocean OGCM. *J. Phys. Oceanogr.,* **37,** 1610–1627.

Lee, T., and I. Fukumori, 2003: Interannual-to-decadal variations of tropical–subtropical exchange in the Pacific Ocean: Boundary versus interior pycnocline transports. *J. Climate,* **16,** 4022–4042.

Lumpkin, R., 2003: Decomposition of surface drifter observations in the Atlantic Ocean. *Geophys. Res. Lett.,* **30,** 1753, doi:10.1029/2003GL017519.

——, and Z. Garraffo, 2005: Evaluating the decomposition of tropical Atlantic drifter observations. *J. Atmos. Oceanic Technol.,* **22,** 1403–1415.

Matei, D., N. Keenlyside, M. Latif, and J. Jungclaus, 2008: Subtropical forcing of tropical Pacific climate and decadal ENSO modulation. *J. Climate,* **21,** 4691–4709.

McPhaden, M. J., and D. X. Zhang, 2002: Slowdown of the meridional overturning circulation in the upper Pacific Ocean. *Nature,* **415,** 603–608.

Melet, A., L. Gourdeau, W. S. Kessler, J. Verron, and J. Molines, 2010a: Thermocline circulation in the Solomon Sea: A modeling study. *J. Phys. Oceanogr.,* **40,** 1302–1319.

——, ——, and J. Verron, 2010b: Variability in the Solomon Sea circulation derived from altimeter sea level data. *Ocean Dyn.,* **60,** 883–900, doi:10.1007/s10236-010-0302-6.

Murray, S., E. Lindstrom, J. Kindle, and E. Weeks, 1995: Transport through the Vitiaz Strait. *WOCE Notes,* Vol. 7, No. 1, U.S. WOCE Office, College Station, TX, 21–23.

Niiler, P. P., 2001: Global ocean circulation observations. *Observing the Oceans in the 21st Century,* C. J. Koblinsky and N. R. Smith, Eds., GODAE Project Office, 307–323.

——, A. S. Sybrandy, K. Bi, P.-M. Poulain, and D. Bitterman, 1995: Measurement of the water-following capability of holey-sock drifters and TRISTAR drifters. *Deep-Sea Res.,* **42,** 1951–1964.

Qiu, B., and S. Chen, 2004: Seasonal modulations in the eddy field of the South Pacific Ocean. *J. Phys. Oceanogr.,* **34,** 1515–1527.

——, ——, and W. Kessler, 2009: Source of the 70-day mesoscale eddy variability in the Coral Sea and the North Fiji Basin. *J. Phys. Oceanogr.,* **39,** 404–420.

Ridgway, K. R., J. S. Godfrey, G. Meyers, and R. Bailey, 1993: Sea level response to the 1986–1987 El Niño-Southern Oscillation event in the western Pacific in the vicinity of Papua New Guinea. *J. Geophys. Res.,* **98** (C9), 16 387–16 395.

Risien, C. M., and D. B. Chelton, 2008: A global climatology of surface wind and wind stress fields from eight years of QuikSCAT scatterometer data. *J. Phys. Oceanogr.,* **38,** 2379–2413.

Ueki, I., Y. Kashino, and Y. Kuroda, 2003: Observations of current variations off the New Guinea coast including the 1997–1998 El Niño period and their relationship with Sverdrup transport. *J. Geophys. Res.,* **108,** 3243, doi:10.1029/2002JC001611.